



Research Article

Molecular Docking Studies of Selected Inhibitors of β -cell Lymphoma-2 Family Proteins

David E. Arthur^{1,*}, Augustina O. Aroh², Stanley I. R. Okoduwa³, Umar T. Mamza¹¹Department of Chemistry, University of Maiduguri, Maiduguri, Nigeria²Department of Chemistry, Ahmadu Bello University, Zaria, Nigeria³Department of Biochemistry, School of Basic Medical Sciences, Babcock University, Ilishan-Remo, Nigeria

OPEN ACCESS ABSTRACT

*CORRESPONDENCE

Arthur, D. E.
eadavid@unimaid.edu.ng
+234-803-918-3847

ARTICLE HISTORY

Received: 26/08/2022

Reviewed: 13/09/2022

Revised: 20/09/2022

Accepted: 05/12/2022

Published: 30/12/2022

CITATION

Arthur, D. E., Aroh, A. O., Okoduwa, S. I. R. and Mamza, U. T. (2022). Molecular Docking Studies of Selected Inhibitors of β -cell Lymphoma 2 Family Proteins. *Nigerian Journal of Biochemistry and Molecular Biology*. 37(4), 241-256

Thirty-six compounds obtained from the PubChem database were used to study the inhibition of BCL-2 receptor through a computational-aided drug-design technique. The molecular docking of all the ligands was evaluated for binding to BCL-2 protein (apoptosis regulator). All the selected chemical datasets were drawn with Chemdraw program and docked within the binding pocket of BCL-2 using ICM-pro molsoft software. The structures of AP7 and AP26 were modified to form new compounds designated AP7a and AP26a respectively. The binding energies of AP7a and AP26a were determined as well as those of the thirty-six lead compounds. Ligands AP7 (-25.313 kcal/mol) and AP26 (-29.430 kcal/mol) were the best of all the 36 compounds. A notable improvement was seen in the binding pose of the modified compounds where the result of the binding energy values of AP7a and AP26a was found to be -25.264 kcal/mol and -26.0851 kcal/mol respectively. The number of hydrogen bonds found in AP7a was significantly more than its parent lead. These bonds were formed between the compound and the following amino acids: ARG139 (2.05Å), TRY180 (1.55Å), LEU59 (1.76Å), GLU135 (2.63Å) and ARG139 (1.82Å). The binding pose of AP26a was found to have seven hydrogen bonds: HIS120 (2.13Å), ARG129 (1.72Å), Leu59 (1.98 Å), SER60 (2.64 Å), LYS58 (2.63), GLN118 (1.95 Å) and THR132 (2.54Å). The aforementioned results showed that the newly designed compounds were better BCL-2 apoptosis regulator inhibitors compared with the 36 compounds used for the study, due to the significant hydrogen bond energies formed by the novel compounds.

Keywords: Cancer, B-cell lymphoma 2 (BCL-2), Docking analysis, Binding affinity

INTRODUCTION

The B-cell lymphoma 2 (BCL-2) protein family is the fundamental gate keepers of the intrinsic or mitochondrial apoptotic reaction. The family encompasses structurally-related proteins with contrasting functions that might prevent apoptosis by intermingling with one another (Adams *et al.*, 2019). The BCL-2 family is naturally classified into three clusters, including anti-apoptotic proteins, pro-apoptotic effectors and pro-apoptotic initiators. The apoptotic-promoting effects from the pro-apoptotic initiators and effectors are opposed by their unswerving interaction with the anti-apoptotic family members. It is this subtle and

active equilibrium amongst the pro- and anti-apoptotic BCL-2 family members that decides whether a B-cell experiences apoptosis or survives.

Interactions amongst the BCL-2 family proteins regulate the ultimate fate of a cell while the nature of interaction with one another to normalize apoptosis remains a disconcerted fundamental issue (Rooswinkel *et al.*, 2014). Until now, the antiapoptotic BCL-2 proteins are assumed to interact with BCL2-Associated X Protein (BAX) weakly, showing that recombinant BCL-2 and BCL-w also known as BCL-2-like

protein 2 (BCL2L2) interacts well with a BCL-2 homology 3 domain-containing peptide (BH3) derived from BAX, and hence showing the dissociation constants of 15 and 23 nM (Adams and Cory, 2001; Ku *et al.*, 2011; Adams *et al.*, 2019; Singh *et al.*, 2019; Warren *et al.*, 2019; Patterson *et al.*, 2021; Zhang *et al.*, 2022). Numerous reports from the literature have shown that the binding affinities between BCL-2 subfamily proteins with BAX are always high. Hence, only a subgroup of BH3-only proteins such as p53 upregulated modulator of apoptosis (PUMA), BCL-2 interacting mediator of cell death (BIM) and abundant proapoptotic protein of the BCL-2 family (BID) are able to inhibit BAX from the antiapoptotic BCL-2 proteins to provoke apoptosis. This suggests that inhibiting BCL-2 protein is essential in activating the apoptotic property of BAX (Antignani and Youle, 2006; Adams *et al.*, 2019; Basu, 2021; Bertram *et al.*, 2022; He *et al.*, 2022).

Computer-Aided Drug Design (CADD) is a potent technique for designing of possible drugs for inhibition of BCL-2 (Enyedy *et al.*, 2001; Brogi, *et al.*, 2020; Arthur *et al.*, 2021; Arthur *et al.*, 2022). This tool has been playing a vital part in predicting the binding energy of synthesized compound which greatly saves time and resources in the cycles of drug study (Thomsen and Christensen, 2006; Brogi, *et al.*, 2020). BCL-2 proteins have been reported in the literature as proteins that inhibit the action of BAX by forming a stable complex with the sub-protein. The inhibition of BAX prevents the regulation of cell growth and in some cases cancer cells, so by disrupting the stability of the BCL-2-

BAX complex, the rate at which cell death is induced increased significantly. This research identifies known inhibitors of BCL-2 proteins in the literature which were recommended for further studies and tries to improve on their BCL-2 inhibitory ability. The goal of this investigation is to create new compounds by performing molecular interaction studies, and evaluate the type of interactions existing between the ligands and the amino acids in binding pocket of BCL-2 receptor.

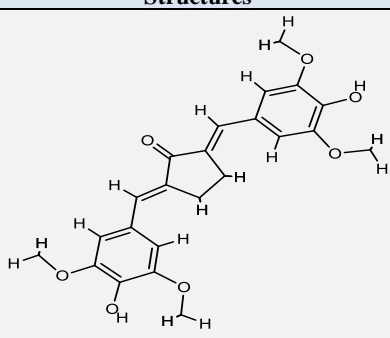
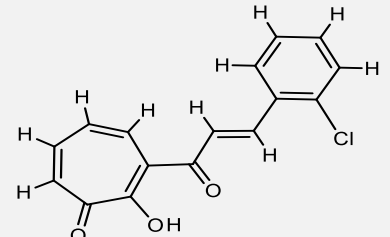
MATERIALS AND METHODS

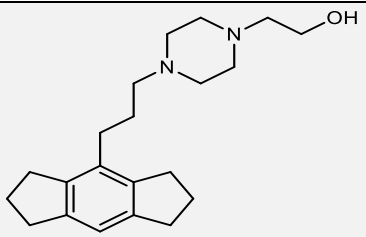
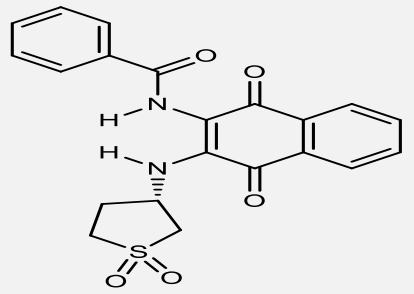
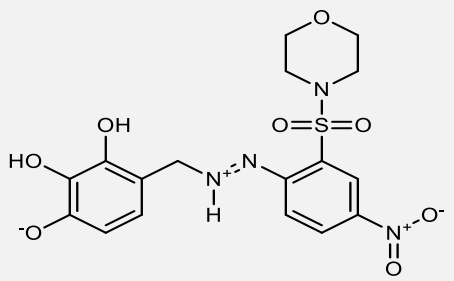
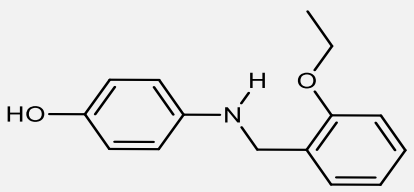
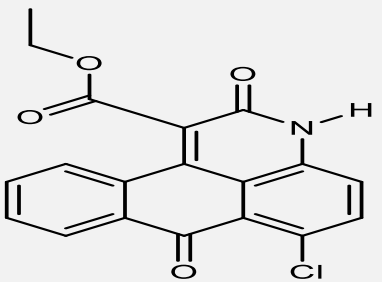
Chemical data set retrieval and activity pre-processing

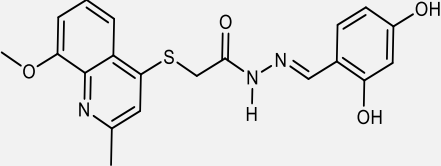
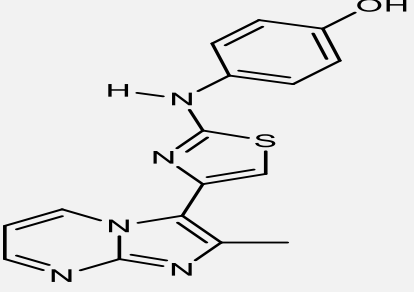
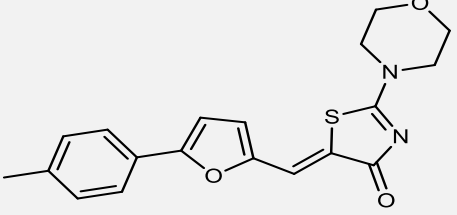
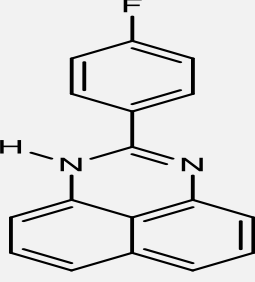
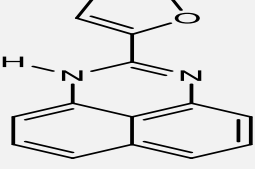
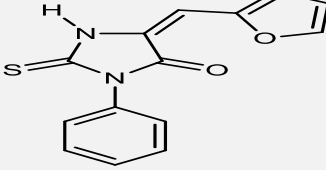
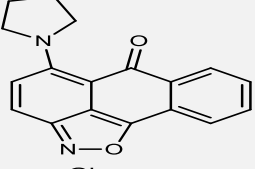
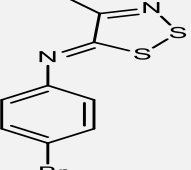
The chemical datasets were selected after curating a series of reported compounds with significant inhibitory activity against the protein BCL-2 (Table 1). The activities of the compounds were reported in 50% effective concentration (EC₅₀) on the PubChem website. The chemical structures of the compounds were confirmed using their PubChem SID and ZincID and in cases where hydrogen atoms were missing, we added the hydrogen atoms before optimizing the structures.

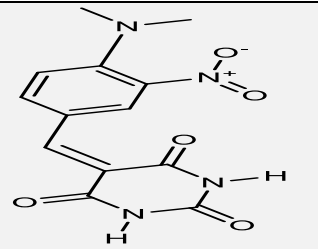
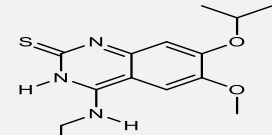
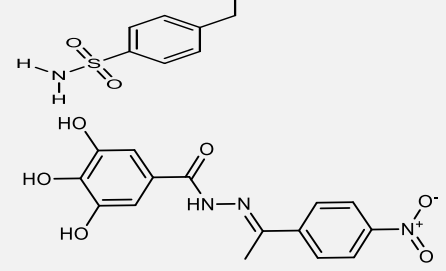
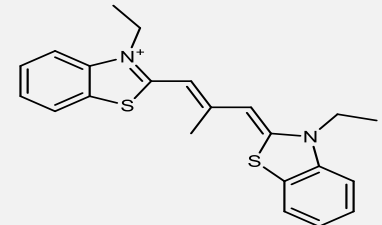
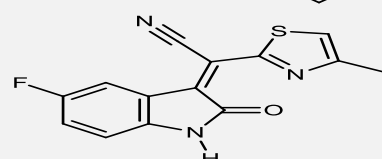
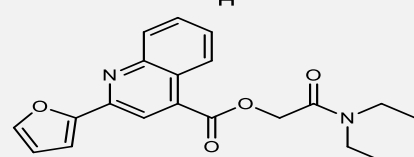
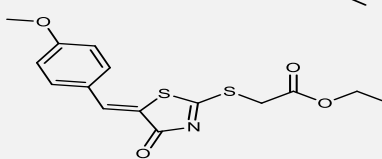
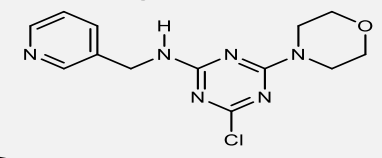
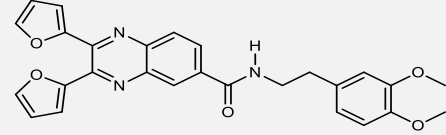
Thirty-six inhibitors of BCL-2 with their corresponding ZincID were retrieved from Pubchem NMLLSC (http://www.bindingdb.org/jsp/dbsearch/PrimarySearch_ki.jsp?energyterm=kJ/mole&tag=pol&polymerid=508&target=Apoptosis+regulator+Bcl-2&column=ki&startPg=0&Increment=50&submit=Search) and are presented in Table 1.

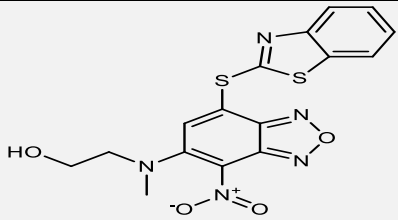
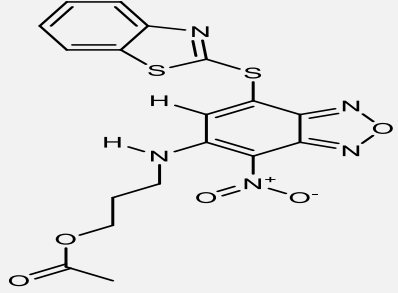
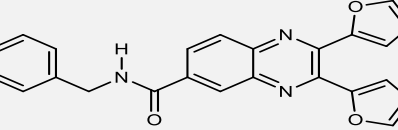
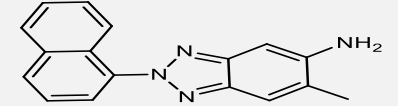
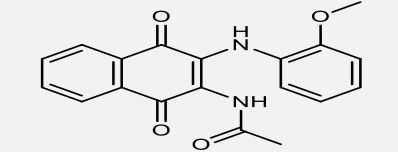
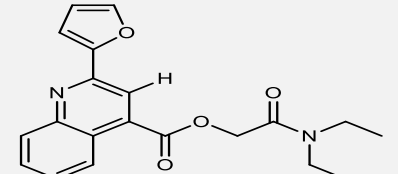
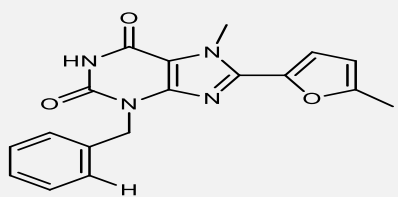
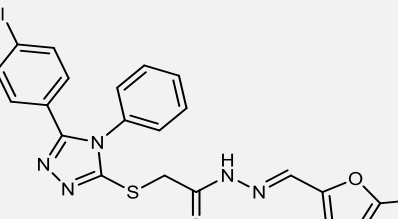
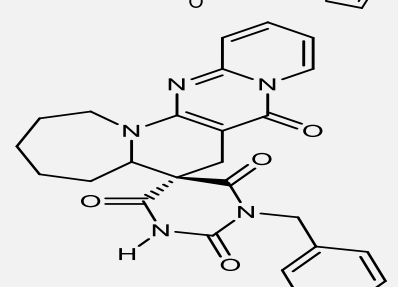
Table 1. Structures and Zinc Identification Number (Zinc ID) of the Chemical Dataset

Name	Structures	Zinc ID of Ligand	PubChem SID	EC ₅₀ (nM)
AP1		ZINC38145472	252,615,754	5,130
AP2		ZINC07089644	252,615,755	14,950

AP3		ZINC19802256	252,615,756	17,850
AP4		ZINC08830252	252,616,283	8,860
AP5		ZINC00707827	252,616,285	15,970
AP6		ZINC25326362	252,616,287	19,650
AP7		ZINC13122352	252,616,290	4,660
AP8		ZINC00359743	252,616,292	3,630
AP9		ZINC11363994	242,052,859	7,650

AP10		ZINC13126047	252,615,757	24,130
AP11		ZINC03998376	252,615,758	670
AP12		ZINC13571887	252,615,759	44,580
AP13		ZINC00310678	252,616,299	9,270
AP14		ZINC00310112	252,616,300	9,760
AP15		None	252,616,301	27,230
AP16		ZINC00265971	242,052,860	27,920
AP17		ZINC12428973	252,616,306	49,760

AP18		ZINC03880366	252,616,314	16,390
AP19		ZINC15953262	252,615,767	540
AP20		ZINC13139536	252,616,320	5,960
AP21		ZINC01627076	252,615,768	22,350
AP22		ZINC60238766	252,615,769	4,560
AP23		ZINC02633911	252,616,328	4,950
AP24		ZINC00342883	252,616,246	2,060
AP25		ZINC00051313	252,615,720	18,880
AP26		ZINC02951107	252,615,712	25,800
AP27		ZINC08667024	252,616,224	1,910

AP28		ZINC08672153	252,616,211	6,350
AP29		ZINC08656557	252,616,225	840
AP30		ZINC01161125	252,616,217	20,650
AP31		ZINC00532766	252,616,187	1,900
AP32		ZINC13685591	252,616,324	12,100
AP33		ZINC02633911	252,616,328	29,460
AP34		ZINC12695462	252,616,327	48,150
AP35		ZINC15989487	252,623,887	12,250
AP36		ZINC09319034	242,053,083	2,250

Ligand preparation

In this study, geometry optimization procedure of the ligands was carried out through the use of density functional theory (DFT). The chemical structures were minimized by Molecular Mechanics Force Field (MM+) count to remove strain energy and ensuring a well-defined conformer relationship among the compounds (Choudhary and Sharma, 2014), before subjecting it to quantum chemical estimations. It is imperative to note that the utilization of electronic density rather than wave capacity for ascertaining the energy, constitutes the base of DFT (Larif *et al.*, 2013) utilizing the B3LYP hybrid functional (Lee *et al.*, 1988; Becke, 1993) and a 6-311G* basis set. This procedure was applied to all other ligands in each of the datasets.

Receptor preparation

The structure of BCL-2 in complex with a BAX BH3 (PDB ID: 2AX0) (Ku *et al.*, 2011) was downloaded from RCSB PDB (www.rcsb.org), with a resolution of 2.70 Å. The PDB file were converted into an ICM-object (I. MolSoft, 2000) deleting the additional water molecules confined in the x-ray structure collected from PDB data bank. All the hydrogen atoms were optimized before the receptor was then subjected to the process of molecular docking treatment.

There are five different interaction potentials that contribute to the overall free binding energy established between the receptor pocket and the docked ligand. These potentials include van der Waals potential for a hydrogen atom probe, van der Waals potential for a heavy-atom probe (generic carbon of 1.7 Å radius), hydrophobic energy terms, optimized electrostatic energy term and loan-pair-based potential, which reflects directional preferences in hydrogen bonding. These energy terms are based on the all-atom vacuum force field ECEPP/3 with added functions to account for solvation free energy, desolvation energy and entropic contribution. It was shown that after each random step, full local minimization greatly improves the efficiency of the procedure. The ICM program relies on global optimization of the entire flexible ligand in the receptor field and combines large-scale random moves of several types with gradient local minimization and a search history mechanism.

The binding free energy term between the studied ligands and the receptor was computed with aid of the ICM scoring function computed using the following parameters (i) The ligand internal energy force-field, (ii) the entropy loss of the ligand between unbound and bound states, (iii) hydrogen bond interactions between the ligand and the receptor, (iv) the difference in polar and non-polar solvation energy

between unbound and bound states, (v) hydrophobic energy, (vi) electrostatic energy, and (vii) desolvation energy.

The receptors after treatment were docked with their respective ligands. Five types of interaction potentials that represents the receptor pocket includes van der Waals potential for a hydrogen atom probe, van der Waals potential for a heavy-atom probe (generic carbon of 1.7 Å radius), optimized electrostatic term, hydrophobic terms and loan-pair-based potential, which reflects directional preferences in hydrogen bonding were calculated. These energy terms are based on the all-atom vacuum force field ECEPP/3 with added functions to account for solvation free energy and entropic contribution. The score was calculated by:

$$G_{\text{bind}} = E_{\text{int}} + T\Delta S_{\text{Tor}} + E_{\text{vw}} + \alpha_1 E_{\text{el}} + \alpha_2 E_{\text{hb}} + \alpha_3 E_{\text{hp}} + \alpha_4 E_{\text{sf}}$$

E_{vw} , E_{el} , E_{hb} , E_{hp} , and E_{sf} are van der Waals, electrostatic, hydrogen bonding, and non-polar and polar atom solvation energy differences between bound and unbound states, respectively. E_{int} is the ligand internal strain, ΔS_{Tor} is its conformational entropy loss upon binding, $T=300$ K, and α_i are ligand and receptor independent constants. Each compound was docked to the protein binding pocket, and a score from the docking was assigned to each compound according to the weighed component of the ICM scoring function. Each compound was docked twenty times to ensure the convergence of the Monte Carlo optimization, and the minimum score of each ligand from the twenty independent docking experiments was retained and used for ranking (Neves *et al.*, 2012).

Template based method as described in literature (Speck-Planche *et al.*, 2012) with modification was used to design new hypothetic molecules in the study. A template molecule was chosen from the dataset having good binding affinity value to serve as a scaffold, after the compound activities have been correlated with their binding affinity determined through molecular docking studies. The compound with the best binding affinity was selected as the lead compound for the design. Using the knowledge gained from interpreting the binding pose of the compound with the receptor active site, different new and synthetically viable molecules are created from the template by insertion, deletion and substitution of different substituent to the original molecules (Table 1).

In this study, result of the ligands docked against the BCL-2 target was reviewed and the interactions of the best inhibitors were discussed. These are the ligands with the lowest binding energy for the active site of the receptor.

The newly designed compounds, when docked, were found with improved binding affinity and, in some instance, its binding energy was far more significant than the lead compound used in the design. This was achieved by introducing some fragments found to bind strongly to the active site of the receptor (Figure 3). The terminal alkoxy groups in AP26 were edited by introducing a more polar hydroxyl substituent in order to increase the hydrogen bond donors of the compound.

Discovery studio software was utilized to view the various ligand-protein interactions in the docked complexes (MolSoft, 2000; L. Molsoft, 2017; Scarpino *et al.*, 2018).

RESULTS AND DISCUSSION

The molecular docking result (MDR) results studies between the ligands and protein target revealed clearly the molecular docking score of each docked ligand associated with docking scores fluctuated from -8.236 to -29.43 kcal/mol presented in Table 2.

Table 2. Quantitative Description of the Interaction of all the Inhibitors and the Newly Designed Compounds on BCL-2 Receptor (PDB ID: 2XA0)

Name	Docking Score (kcal/mol)	nflex	Hbond	Hphob	VwInt	Eintl	Dsolv	SoIEI
AP1	-19.1839	0	-4.25178	-6.06911	-28.4973	9.36455	17.0655	17.1782
AP2	-22.5993	0	-5.01071	-5.02741	-24.8127	4.35919	12.7071	13.2251
AP3	-12.2894	7	-3.63271	-6.01408	-24.1169	7.88586	13.6059	16.1261
AP4	-16.217	2	-0.83493	-8.15214	-38.1406	24.2469	18.1533	22.2468
AP5	-23.2244	1	-4.63281	-6.29669	-29.1479	6.46277	15.3523	14.7712
AP6	-23.0238	2	-3.45966	-5.7886	-31.5922	8.27078	12.6221	15.9592
AP7	-25.3126	5	-8.84507	-4.03962	-26.0643	14.3199	17.6066	14.5928
AP8	-11.2375	3	-1.15287	-6.18715	-25.5848	4.51393	11.6717	16.448
AP9	-15.0923	1	-3.54192	-4.59719	-26.1572	7.94646	16.5638	15.2776
AP10	-12.8385	2	-4.96248	-6.27639	-34.9472	18.2745	25.6769	27.8958
AP11	-16.9413	0	-4.30778	-4.63377	-25.93	3.92856	17.7666	14.6472
AP12	-21.2719	1	-6.73187	-7.34105	-25.5262	10.9368	16.9591	19.523
AP13	-9.60397	1	-0.39287	-5.11034	-24.0434	2.67574	11.6229	14.4547
AP14	-8.23606	0	-1.08036	-4.70566	-21.9237	1.84427	12.552	15.3935
AP15	-12.9137	1	-2.43079	-4.62361	-25.0664	14.4732	12.9813	16.7644
AP16	-16.6164	0	-4.29659	-5.77409	-20.6268	9.39156	12.1088	14.6482
AP17	-9.1109	1	-1.40093	-3.7066	-22.1287	1.52758	15.1248	10.7605
AP18	-19.9553	1	-3.53195	-4.13415	-25.9201	6.33535	13.2243	10.8368
AP19	-16.2838	5	-2.84761	-4.84912	-32.1085	4.09147	14.8887	18.3508
AP20	-19.9559	2	-5.71831	-4.1088	-21.2631	11.9937	16.4428	7.56869
AP21	-14.7562	2	0	-6.90892	-26.6328	3.61013	10.5931	11.1527
AP22	-14.4093	0	-4.28132	-4.97902	-21.4753	4.31449	12.9925	17.408
AP23	-11.8037	5	-1.28253	-6.94034	-27.4869	6.92271	14.612	14.5743
AP24	-17.5128	3	-5.13241	-6.16796	-29.7359	6.93205	20.7308	18.1704
AP25	-23.9964	2	-6.84131	-5.68611	-23.5797	9.29524	16.8239	10.4297
AP26	-29.4300	3	-7.06635	-8.25467	-35.801	13.2296	19.969	19.7011
AP27	-18.3383	5	-3.90243	-5.39874	-29.8007	10.202	17.599	13.2627
AP28	-15.6870	4	-4.49081	-5.34106	-21.9947	8.78475	16.0821	10.2823
AP29	-12.2600	5	-3.87003	-5.30177	-30.9159	10.1553	20.2371	20.9416
AP30	-21.9785	2	-5.67945	-6.78412	-30.098	9.2371	16.4602	20.4376
AP31	-8.38361	0	-1.27321	-4.96523	-23.4919	7.00361	14.8506	15.9367
AP32	-25.5953	0	-3.83969	-5.41884	-25.6274	8.46542	12.2219	6.37992

AP33	-12.0887	5	-2.89676	-7.24918	-30.4351	4.77946	15.2967	24.3327
AP34	-17.2014	2	-3.20269	-5.40108	-29.3712	6.81874	15.845	16.375
AP35	-12.9411	4	-4.2248	-7.2384	-29.7805	18.8068	21.2305	21.2955
AP36	-16.8692	2	-4.94668	-5.40411	-29.118	7.90161	19.7496	18.7461
AP7a	-25.2638	7	-8.76144	-3.23859	-27.6261	13.0381	20.075	11.2763
AP26a	-26.0851	3	-9.78996	-7.34077	-36.622	21.7286	23.6255	31.3707

Nflex: - Number of rotatable torsions, Hbond: - hydrogen bond energy, Hphob: - hydrophobic energy in exposing a surface to water, Vwint: - The van der Waals interaction energy (sum of gc and gh van der Waals), Eintl: - Internal conformational energy of the ligand, Dsolv: - The desolvation of exposed H-bond donors and acceptors, SolEl: - The solvation electrostatics energy change upon binding

The molecular docking scores are a depiction of the free energy of binding which are broken down in bits outlined by a set of contributing factors shown in Table2. The binding energy is reported in kcal/mol and the values found less than -20kcal/mol have been reported by other sources to be less potent due to their low stability in the binding pockets and low contributing factor of the hydrogen bonds between any receptor and the inhibitor (Thomsen and Christensen, 2006; Adeniji *et al.*, 2020; Arthur *et al.*, 2022). Compounds with less than 3 number of flexible bonds (nflex) but impressive binding affinity can be used as a lead compound in designing better drug candidates, since they satisfy the rule of five theory (Thomsen and Christensen, 2006; Scarpino *et al.*, 2018; Tinworth and Young, 2020).

Ligand AP26 was reported with the lowest binding energy of -29.43kcal/mol in Table2. The value of the binding energy was found to be significant because of the large contribution of hydrophobic interaction energy (-8.25467 kcal/mol) to the value compared to the hydrogen bond energy (-7.06635 kcal/mol) contribution. This contribution shows that the overall Gibbs free energy was largely determined by entropic forces and so the complex stability maybe threatened under some specific thermodynamic system. Ligand AP7 was also identified as a potential lead molecule in designing other more active inhibitors of BCL-2 apoptosis regulator. The 2D-interaction of AP7 and BCL-2 receptor is shown in Figure1, while that for AP26 can be seen in Figure 2.

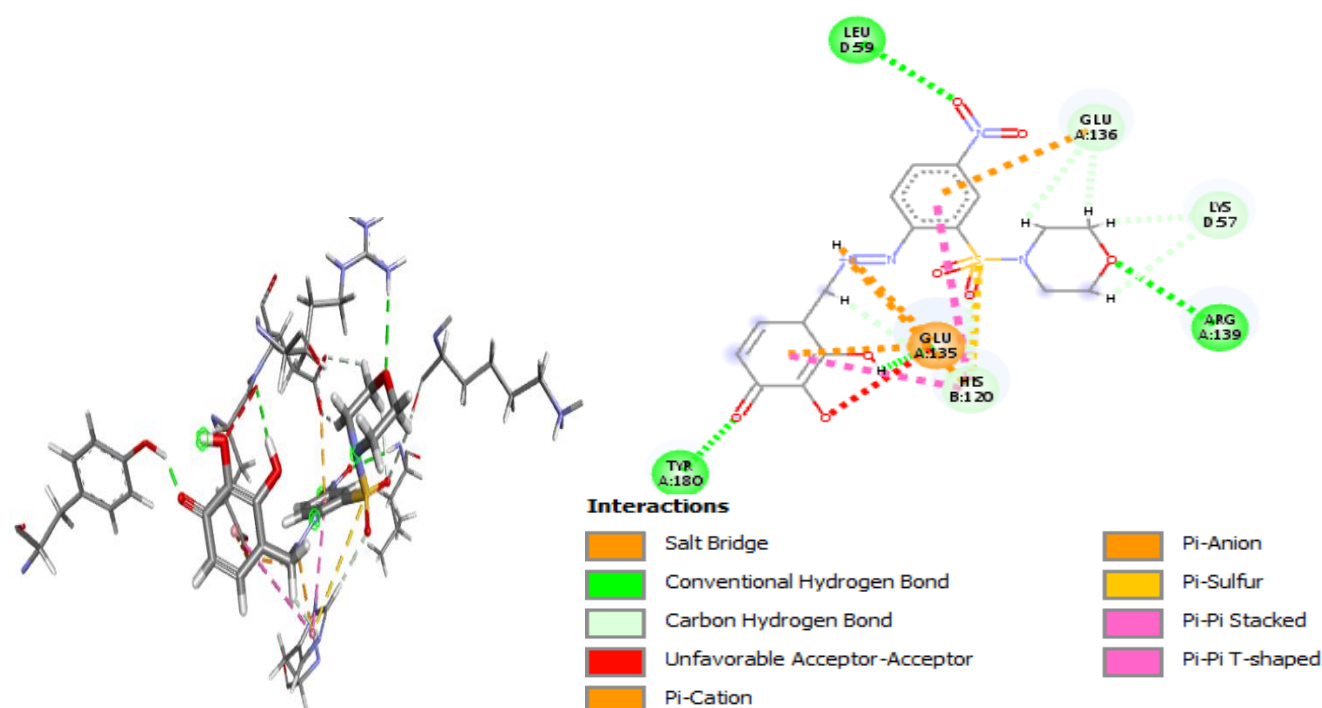


Figure 1. 2D and 3D Views of AP7 with Surrounding Amino Acids of BCL-2 (2XA0)

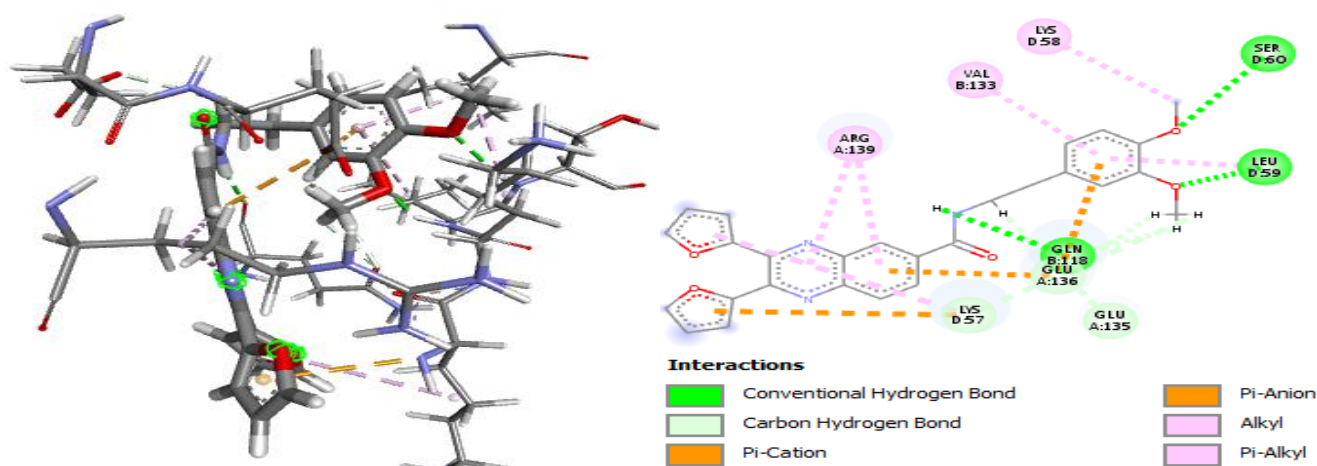


Figure 2. The 2D and 3D Views of AP26 with Surrounding Amino Acids of BCL-2 (2XA0)

The binding energy of AP7 was higher than that for AP26, but its interaction with the binding pocket of BCL-2 receptor shows it has a lesser binding energy than any of the other 34 compounds that were looked into. The binding energy of AP7 presented in Table 2 is given as -25.3126 kcal/mol, while the hydrogen bond energy and hydrophobic bond energy were presented as -8.845 and -4.039 kcal/mol respectively. The contribution of the hydrogen bonds suggests the complex will be held tightly in the binding pocket of the receptor.

Table 3 shows the details of the interaction between AP7 and BCL-2 receptor. The amino acids shown in Figure 1 interacting with the ligand is displayed in Table 3. Four hydrogen bonds were found between the ligand and the amino acids (Arg139, Tyr180, Leu59 and Glu135) in the binding pocket, but Tyr180 was most significant. This hydrogen bond was reported with a bond distance of 1.49 Å, and was found to be donated by Tyr180 to the carbonyl oxygen of the cyclohexene fragment of compound AP7. Other significant interactions such as Π -cation, Π -Sulphur, π - π stacked and π - π T-shaped bonds were found between the AP7 and His102 of chain B in 2AX0 receptor.

Table 3. Interaction Types and Amino Acids Involved in the Inhibition of BCL-2 Receptor (PDB ID: 2XA0) with AP7 Inhibitor

Bond Distance	Bond Type	Bond-Donor Species	Bond-Donor Type	Bond-Acceptor Species	Bond-Acceptor type
2.29	Salt Bridge; Attractive Charge	AP7 (H3)	HB-Donor; Positive	A:GLU135:OE1	HB-Acceptor; Negative
2.53	Hydrogen Bond	A:ARG139:HH11	HB-Donor	AP7:O1	HB-Acceptor
1.49	Hydrogen Bond	A:TYR180:HH	HB-Donor	AP7:O8	HB-Acceptor
2.54	Hydrogen Bond	D:LEU59:HN	HB-Donor	AP7:O4	HB-Acceptor
2.51	Hydrogen Bond	AP7:H1	HB-Donor	A:GLU135:O	HB-Acceptor
2.36	Carbon Hydrogen Bond	B:HIS120:HE1	HB-Donor	AP7:O2	HB-Acceptor
2.79	Carbon Hydrogen Bond	AP7:H10	HB-Donor	D:LYS57:O	HB-Acceptor
2.65	Carbon Hydrogen Bond	AP7:H10	HB-Donor	AP7:O3	HB-Acceptor
2.42	Carbon Hydrogen Bond	AP7:H15	HB-Donor	B:HIS120:NE2	HB-Acceptor
2.39	Carbon Hydrogen Bond	AP7:H6	HB-Donor	A:GLU136:OE1	HB-Acceptor
2.46	Carbon Hydrogen Bond	AP7:H8	HB-Donor	A:GLU136:OE2	HB-Acceptor
1.94	Carbon Hydrogen Bond	AP7:H9	HB-Donor	D:LYS57:O	HB-Acceptor
2.55	Carbon Hydrogen Bond	AP7:H9	HB-Donor	AP7:O3	HB-Acceptor
3.10	Π -Cation	AP7:N3	Positive	B:HIS120	Π -Orbitals
3.44	Π -Anion	A:GLU135:OE1	Negative	AP7	Π -Orbitals
3.36	Π -Anion	A:GLU136:OE1	Negative	AP7	Π -Orbitals
5.44	Π -Sulfur	AP7:S1	Sulfur	B:HIS120	Π -Orbitals
4.83	Π - π Stacked	B:HIS120	Π -Orbitals	AP7	Π -Orbitals
5.86	Π - π T-shaped	B:HIS120	Π -Orbitals	AP7	Π -Orbitals

Compounds AP12, AP7, AP25 and AP26 were considered the best inhibitors on the bases of their hydrogen bonds contribution, the values were reported for each molecule in the Tables as -6.731, -8.845, -6.841 and -7.066 kcal/mol respectively. The cut-off point for the hydrogen bond energy was -6.0 kcal/mol. The topmost two compounds were selected after comparing the binding energy of all four compounds. The values of AP26 and AP7 were close but significantly lower in binding energy than that of AP12 and AP7.

The hydrogen bond energy helps stabilize the conformation of the complex formed (Zhang, 2009). The lower the

hydrogen bond energy the more the number of hydrogen bonds formed between the compound and the active site of the BCL-2 receptor, thereby increasing the stability of the formed complex (Phillips *et al.*, 2020).

Table4 shows the interaction types found between AP26 ligand and the receptor binding pocket. The table shows that only three hydrogen bonds were formed in the complex. They were donated by the amino group of Leu59 and Ser60 of the receptor to the alkoxy oxygen atom found in AP26, just as shown in 2d structure of the complex in Figure2.

Table 4. Interaction Types and Amino Acids Involved in the Inhibition of BCL-2 Receptor (PDB ID: 2XA0) with AP26 Inhibitor

Bond Distance	Bond Type	Bond-Donor Species	Bond-Donor type	Bond-Acceptor Species	Bond-Acceptor type
1.52	Hydrogen Bond	D:LEU59:HN	HB-Donor	:AP26:O3	HB-Acceptor
2.46	Hydrogen Bond	D:SER60:HN	HB-Donor	:AP26:O4	HB-Acceptor
2.01	Hydrogen Bond	:AP26:H1	HB-Donor	B:GLN118:O	HB-Acceptor
2.63	Carbon Hydrogen Bond	:AP26:H18	HB-Donor	D:LYS57:O	HB-Acceptor
2.52	Carbon Hydrogen Bond	:AP26:H19	HB-Donor	B:GLN118:OE1	HB-Acceptor
2.26	Carbon Hydrogen Bond	:AP26:H20	HB-Donor	A:GLU136:OE1	HB-Acceptor
3.03	Carbon Hydrogen Bond	:AP26:H5	HB-Donor	A:GLU135:OE2	HB-Acceptor
3.49	Π -Cation	D:LYS57:N	Positive	:AP26	Π -Orbitals
4.00	Π -Anion	A:GLU136:OE1	Negative	:AP26	Π -Orbitals
3.52	Π -Anion	A:GLU136:OE1	Negative	:AP26	Π -Orbitals
4.04	Alkyl	:AP26:C27	Alkyl	D:LYS58	Alkyl
5.23	Π -Alkyl	:AP26	Π -Orbitals	D:LYS57	Alkyl
5.47	Π -Alkyl	:AP26	Π -Orbitals	A:ARG139	Alkyl
4.72	Π -Alkyl	:AP26	Π -Orbitals	B:VAL133	Alkyl
4.55	Π -Alkyl	:AP26	Π -Orbitals	D:LEU59	Alkyl
5.33	Π -Alkyl	:AP26	Π -Orbitals	A:ARG139	Alkyl

Designing the novel compounds

The set of compounds (AP7 and AP26) with the best binding affinity for the binding pocket were selected and structurally modified or optimized to improve the fastness and stability of the compounds to that binding pocket (Arthur *et al.*, 2018). The new compounds designed are presented in Figure3 as AP7a and AP26a respectively. The structure of AP7 was modified by introducing two amine groups and two hydroxyl groups to the structure, so as to further increase the hydrogen bonds found in AP7-2AX0 complex. While the structure of AP26a was formed by converting the alkoxy

groups and introducing hydroxyl groups to AP26a. The basis for converting the alkoxy group to hydroxyl group is to make that part or area of the molecule more polar, hence increasing the chances of that fragment to form two types of hydrogen bonds. These bonds include a hydrogen bond donor from the hydrogen atom of the hydroxyl group and a hydrogen bond acceptor from the oxygen atom of the hydroxyl group. This little change was found to be significant to the number of hydrogen bonds formed by the modified molecule, since the number of hydrogen bond increased as confirmed by the result.

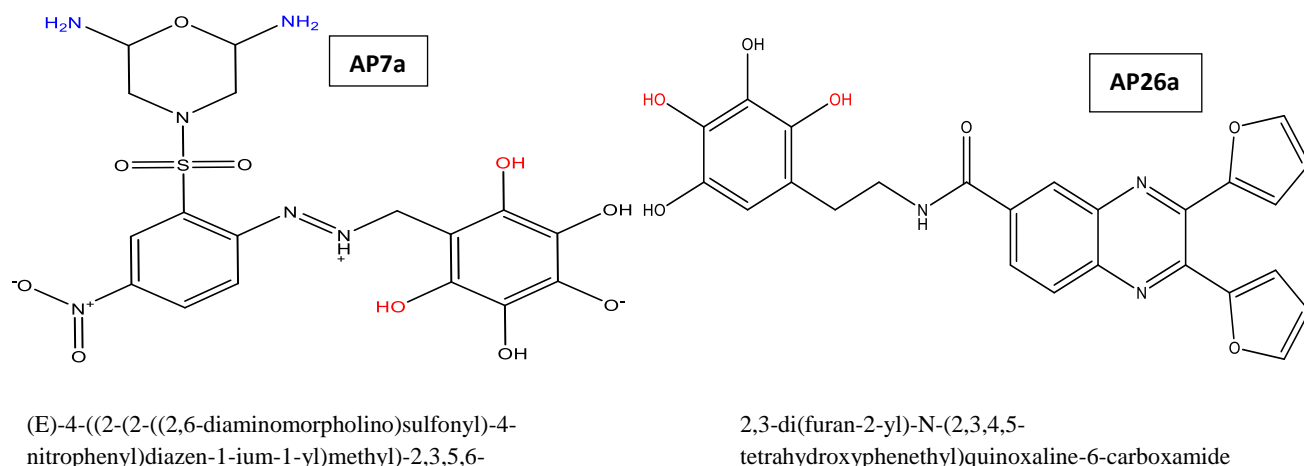


Figure 3. The 2-D Structures of the Newly Designed Compounds (AP7a and AP26a) with their IUPAC Names

The docking result of the newly designed compounds shows improvement in the binding pose of the lead molecules AP7 and AP26, that were used as a template for their design. The results presented in the Tables confirm increase in hydrogen bonds formation and the decrease in hydrophobic interactions between the newly designed molecules with the amino acids found in the binding pocket. The result shows that the changes lead to the reduction in entropic contributions made initially to the Gibbs free energy of binding for the lead molecules (AP26 and AP7).

The molecular docking result for AP7a and AP26a are presented in Tables 5 and 6 respectively, while the best binding pose of these ligands extracted from the docking study was presented in Figures 5 and 6 for AP7a and AP26a respectively.

Figure 4 shows the 2D and 3D structures of ligand AP7a and some of the amino acids found within the binding pocket of the receptor. The figure shows the conventional hydrogen bonds formed between the ligand and Lue59, Arg139 and Tyr180. Other notable interactions that can be seen from the figure include a Pi-Cation and Pi-Anion interactions which are differentiated by their bright orange colour. Figure 5 shows the binding pose of AP26a with some amino acids. The figure shows seven amino acids forming conventional hydrogen bonds with the ligand. Five conventional hydrogen bonds were formed between 2,3,4,5-tetrahydroxyphenyl group of the ligand and Arg129, Gln118, His120, Thr132 and Leu59. While the remaining two amino acids (Ser60, Lys58) donate hydrogen bond to the oxo side of the carboxamide group.

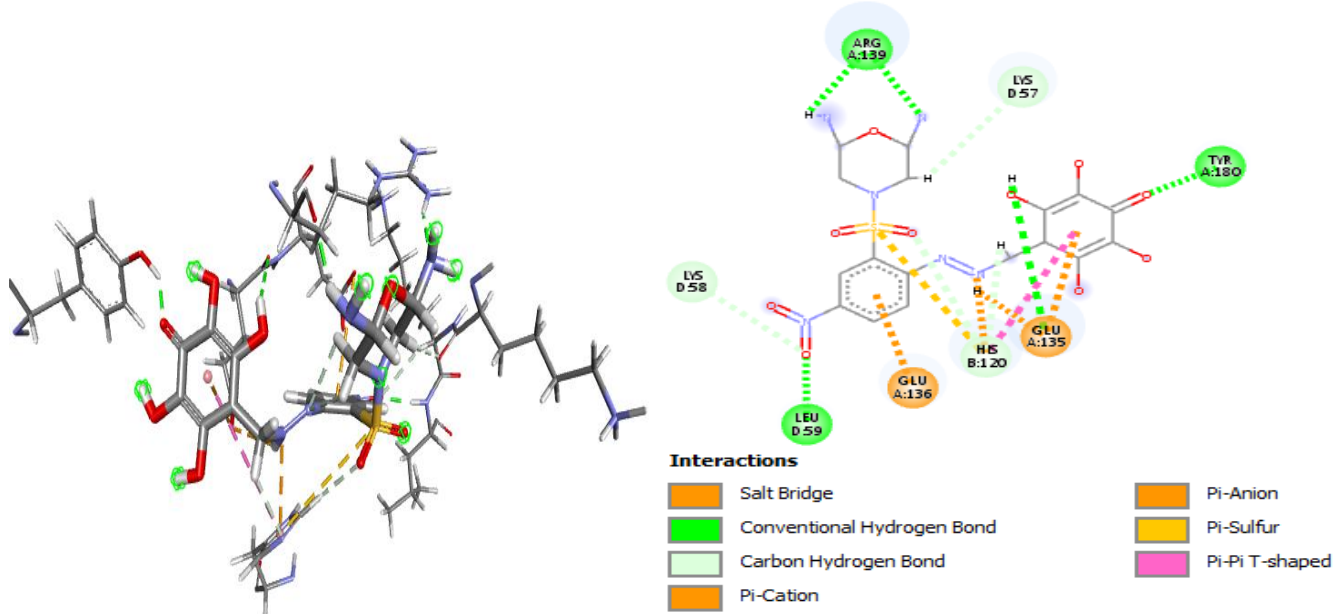


Figure 4. The 2D and 3D Views of AP7a with Surrounding Amino Acids of BCL-2 (2XA0)

Table 5. Interaction Types and Amino Acids Involved in the Inhibition of BCL-2 Receptor (PDB ID: 2XA0) with AP7a Inhibitor

Bond Distance	Bond Type	Bond-Donor Species	Bond-Donor type	Bond-Acceptor Species	Bond-Acceptor type
2.85	Salt Bridge; Attractive Charge	:AP7a:H3	HB-Donor; Positive	A:GLU135:OE1	HB-Acceptor; Negative
2.05	Hydrogen Bond	A:ARG139:HH11	HB-Donor	:AP7a:N5	HB-Acceptor
1.55	Hydrogen Bond	A:TYR180:HH	HB-Donor	:AP7a:O8	HB-Acceptor
1.76	Hydrogen Bond	D:LEU59:HN	HB-Donor	:AP7a:O4	HB-Acceptor
2.63	Hydrogen Bond	:AP7a:H1	HB-Donor	A:GLU135:O	HB-Acceptor
1.82	Hydrogen Bond	:AP7a:H17	HB-Donor	A:ARG139:O	HB-Acceptor
2.59	Carbon Hydrogen Bond	B:HIS120:HE1	HB-Donor	:AP7a:O2	HB-Acceptor
2.73	Carbon Hydrogen Bond	D:LYS58:HA	HB-Donor	:AP7a:O4	HB-Acceptor
2.63	Carbon Hydrogen Bond	:AP7a:H13	HB-Donor	B:HIS120:NE2	HB-Acceptor
2.81	Carbon Hydrogen Bond	:AP7a:H4	HB-Donor	:AP7a:N2	HB-Acceptor
2.81	Carbon Hydrogen Bond	:AP7a:H5	HB-Donor	:AP7a:N2	HB-Acceptor
2.60	Carbon Hydrogen Bond	:AP7a:H6	HB-Donor	D:LYS57:O	HB-Acceptor
3.33	Π -Cation	:AP7a:N3	Positive	B:HIS120	Π -Orbitals
3.60	Π -Anion	A:GLU135:OE1	Negative	AP7a	Π -Orbitals
4.75	Π -Anion	A:GLU136:OE2	Negative	AP7a	Π -Orbitals
5.64	Π -Sulfur	:AP7a:S1	Sulfur	B:HIS120	Π -Orbitals
5.91	Π - π T-shaped	B:HIS120	Π -Orbitals	AP7a	Π -Orbitals

Table 5 shows there are a total of five conventional hydrogen bonds formed between AP7a and the amino acids Arg139, Tyr180, Leu59 and Glu135. Arg139 acted as both a hydrogen bond donor and a hydrogen bond acceptor. The Pi-

Pi, Pi-Cation, Pi-anion and Pi-sulfur bonds formed in AP7a-receptor complex were found to be important since they also assist in stabilizing the binding pose of the ligand via intercalation.

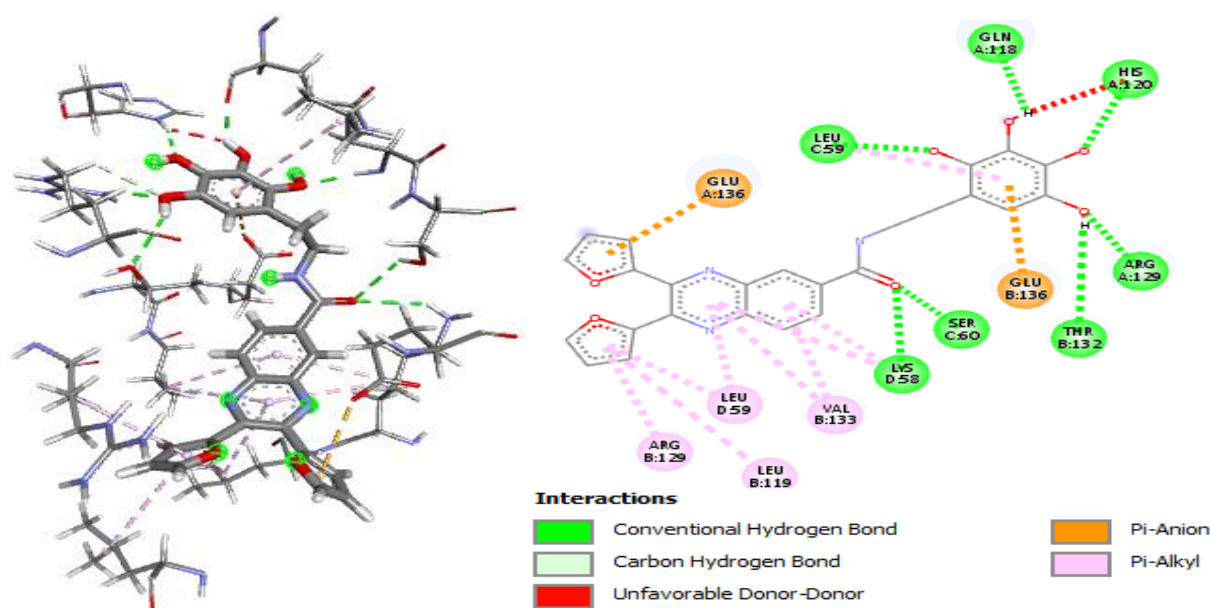
**Figure 5.** The 2D and 3D Views of Interaction Type of AP7a with Surrounding Amino Acids of 2XA0

Table 6. Interaction Types and Amino Acids Involved in the Inhibition of BCL-2 Receptor (PDB ID: 2XA0) with AP26a Inhibitor

Bond Distance	Bond Type	Bond-Donor Species	Bond-Donor type	Bond-Acceptor Species	Bond-Acceptor type
2.13	Hydrogen Bond	A:HIS120:HD1	HB-Donor	:AP26a:O4	HB-Acceptor
1.72	Hydrogen Bond	A:ARG129:HH11	HB-Donor	:AP26a:O7	HB-Acceptor
1.98	Hydrogen Bond	C:LEU59:HN	HB-Donor	:AP26a:O6	HB-Acceptor
2.64	Hydrogen Bond	C:SER60:HG	HB-Donor	:AP26a:O5	HB-Acceptor
2.63	Hydrogen Bond	D:LYS58:HZ3	HB-Donor	:AP26a:O5	HB-Acceptor
1.95	Hydrogen Bond	:AP26a:H16	HB-Donor	A:GLN118:O	HB-Acceptor
2.54	Hydrogen Bond	:AP26a:H19	HB-Donor	B:THR132:OG1	HB-Acceptor
2.79	Carbon Hydrogen Bond	A:ARG129:HD2	HB-Donor	:AP26a:O7	HB-Acceptor
3.26	Π -Anion	A:GLU136:OE1	Negative	:AP26a	Π -Orbitals
4.29	Π -Anion	B:GLU136:OE2	Negative	:AP26a	Π -Orbitals
5.09	Π -Alkyl	:AP26a	Π -Orbitals	B:VAL133	Alkyl
5.06	Π -Alkyl	:AP26a	Π -Orbitals	D:LYS58	Alkyl
4.98	Π -Alkyl	:AP26a	Π -Orbitals	D:LEU59	Alkyl
5.07	Π -Alkyl	:AP26a	Π -Orbitals	C:LEU59	Alkyl
5.03	Π -Alkyl	:AP26a	Π -Orbitals	B:VAL133	Alkyl
4.57	Π -Alkyl	:AP26a	Π -Orbitals	D:LYS58	Alkyl
5.35	Π -Alkyl	:AP26a	Π -Orbitals	B:LEU119	Alkyl
4.50	Π -Alkyl	:AP26a	Π -Orbitals	B:ARG129	Alkyl
5.26	Π -Alkyl	:AP26a	Π -Orbitals	D:LEU59	Alkyl

Seven conventional hydrogen bonds between AP26a and the surrounding amino acids were presented in table 6. Five of these bonds were donated by the amino acids His120, Arg129, Leu59, Ser60 and Lys58, while the remaining two hydrogen bonds were accepted by Gln118 and Thr132. The strongest conventional hydrogen bond was formed between Arg129 and the hydroxyl group of AP26a. The strength of the bond was qualitatively evaluated from the length of the bond, which was presented in table 6 as the shortest of all conventional hydrogen bonds presented. Other notable interactions presented in table 6 include two Pi-anion bonds (Glu136) and nine Pi-alkyl bonds (Leu59, Arg129, Leu119, Lys58, Val133).

In AP7 four hydrogen bonds were formed between the ligand and amino acids Arg139(2.53 Å), Try180(1.49 Å), Leu59(2.54 Å) and Glu135(2.51 Å). While in AP7a five hydrogen bonds are formed with Arg139 (2.05 Å), Tyr180(1.55 Å), Leu59(1.79 Å), Glu135(2.63 Å) and Arg139 (1.82 Å). The result shows that by adding more hydroxyl groups to the trihydroxybenzyl part of AP7 and two amine group to the morpholine part, the modified

structure of AP7 (AP7a) formed more hydrogen bonds that are stronger than those seen in AP7. The result further shows that by introducing those groups, the hydrophobic nature of ligand AP7 in the binding pocket was reduced, thereby enabling the formation of stronger hydrogen bond between AP7a in the binding space. While in AP26 the changes made were significantly more reflected in the number of hydrogen bonds formed compared with that of AP7 and AP26. The two alkoxy group on AP26 were replaced with hydroxyl group. This modification led to a significant increase in the number of hydrogen bonds formed and it also increased the hydrophobic bond energy from -8.255 kcal/mol in AP26 to -7.340 kcal/mol in AP26a, while the hydrogen bond energy was reduced from -7.066 to -9.790 kcal/mol.

The results also show that three hydrogen bonds were formed with amino acids Leu59(1.52 Å), Ser60(2.45 Å) and Gln118(2.01 Å) in AP26. While in AP26a seven hydrogen bonds were formed with the amino acids His120(2.13 Å), Arg129(1.72 Å), Leu59(1.98 Å), Ser60 (2.64 Å), Lys58(2.63 Å), Gln118(1.95 Å) and Thr132(2.54 Å). This shows that by replacing the alkoxy group with hydroxy groups on the

benzene ring, the number of hydrogen bonds formed were significantly increased thereby improving the binding affinity and the stability of AP26a-receptor complex.

CONCLUSION

Molecular docking of all the ligands was done including the newly designed inhibitors termed as AP7a and AP26a. Key features of the docking study were used to evaluate and conclude on the potency of the selected compounds. These features which includes the values of the binding energy and the hydrogen bond contribution to the binding affinity serves as a guide or the basis for making our selections.

AUTHORS' CONTRIBUTIONS

Author DEA got the concept, design the study and participated in data acquisition. Authors SIRO and DEA participated in literature management, data generation, computation and manuscript draft. Authors AOA and UTM contributed equally in data analysis. Authors SIRO and DEA curate the data and revised the manuscript for important content. All the authors approved the final version of the manuscript for publication.

FUNDING STATEMENT

This research did not receive any specific grant from funding agencies in the public, commercial, or not-for-profit sectors.

CONFLICT OF INTEREST

The authors declare that there is no conflict of interest.

ACKNOWLEDGEMENT

None

REFERENCES

- Abdullahi, M., Uzairu, A., Shallangwa, G. A., Arthur, D. E., Umar, B. A., and Ibrahim, M. T. (2020). Virtual molecular docking study of some novel carboxamide series as new anti-tubercular agents. *European Journal of Chemistry*, 11(1), 30-36.
- Adams, C. M., Clark-Garvey, S., Porcu, P., and Eischen, C. M. (2019). Targeting the Bcl-2 family in B-cell lymphoma. *Frontiers in Oncology*, 8, 636.
- Adams, J. M., and Cory, S. (2001). Life-or-death decisions by the Bcl-2 protein family. *Trends in Biochemical Sciences*, 26(1), 61-66.
- Adeniji, S. E., Arthur, D. E., and Oluwaseye, A. (2020). Computational modeling of 4-phenoxy nicotinamide and 4-phenoxy pyrimidine-5-carboxamide derivatives as potent anti-diabetic agent against Tgr5 receptor. *Journal of King Saud University-Science*, 32(1), 102-115.
- Antignani, A., and Youle, R. J. (2006). How do bax and bak lead to permeabilization of the outer mitochondrial membrane? *Current Opinion in Cell Biology*, 18(6), 685-689.
- Arthur, D. E. (2019). Molecular docking studies of some topoisomerase ii inhibitors: implications in designing of novel anticancer drugs. *Radiology of Infectious Diseases*, 6(2), 68-79.
- Arthur, D. E. and Uzairu, A. (2018). Molecular docking study and structure-based design of novel camptothecin analogues used as topoisomerase I inhibitor. *Journal of the Chinese Chemical Society*, 65(10), 1160-1178.
- Arthur, D. E., Akoji, J. N., Sahnoun, R., Okafor, G. C., Abdullahi, K. L., Abdullahi, S. A., and Mgbemena, C. (2021). A theoretical insight in interactions of some chemical compounds as mtor inhibitors. *Bulletin of the National Research Centre*, 45(1), 1-12.
- Arthur, D. E., Elegbe, B. O., Aroh, A. O., and Soliman, M. (2022). Computational drug design of novel covid-19 inhibitor. *Bulletin of the National Research Centre*, 46(1), 1-29.
- Basu, A. (2021). The interplay between apoptosis and cellular senescence: bcl-2 family proteins as targets for cancer therapy. *Pharmacology and Therapeutics*, 230, 107943.
- Becke, A. D. (1993). Density-functional thermochemistry. iii. the role of exact exchange. *Journal of Chemical Physics*, 98(7), 5648-5652.
- Bertram, K., Leary, P. J., Boudesco, C., Fullin, J., Stirn, K., Dalal, V., Zenz, T., Tzankov, A. and Müller, A. (2022). Inhibitors of Bcl-2 and Bruton's tyrosine kinase synergize to abrogate diffuse large B-cell lymphoma growth *in vitro* and in orthotopic xenotransplantation models. *Leukemia*, 36(4), 1035-1047.
- Broggi, S., Ramalho, T.C., Kuca, K., Medina-Franco, J.L. and Valko, M. (2020). *In silico* methods for drug design and discovery. *Frontiers in Chemistry*, 8, 612
- Choudhary, M. and Sharma, B. K. (2014). Qsar Rationales for the 5-Ht6 Antagonistic activity of epiminocyclohepta [B] Indoles. *Journal of Pharmaceutical Chemistry*, 6, 321-330.
- Enyedy, I. J., Ling, Y., Nacro, K., Tomita, Y., Wu, X., Cao, Y., Guo, R., Li, B., Zhu, X., Huang, Y., Long, Y. Q., Roller, P. P., Yang, D. and Wang, S. (2001). Discovery of small-molecule inhibitors of Bcl-2 through structure-based computer screening. *Journal of Medicinal Chemistry*, 44(25), 4313-4324.
- He, W., Li, X., Morsch, M., Ismail, M., Liu, Y., Rehman, F. U., Zhang, D., Wang, Y., Zheng, M., Chung, R., Zou, Y., & Shi, B. (2022). Brain-targeted codelivery of Bcl-2/Bcl-xl and Mcl-1 inhibitors by biomimetic nanoparticles for orthotopic glioblastoma therapy. *ACS Nano*, 16(4), 6293-6308.
- Ku, B., Liang, C., Jung, J. U., and Oh, B.-H. (2011). Evidence that Inhibition of BAX activation by Bcl-2 involves its tight and preferential interaction with the Bh3 domain of BAX. *Cell Research*, 21(4), 627-641.

- Larif, M., Chtita, S., Adad, A., Hmamouchi, R., Bouachrine, M., and Lakhlifi, T. (2013). Predicting biological activity of anticancer molecules 3-Ary L-4-hydroxyquinolin-2-(1h)-One by Dft-Qsar Models. *International Journal of Cancer*, 3(12).
- Lee, C., Yang, W. and Parr, R. G. (1988). Development of the Colle-Salvetti correlation-energy formula into a functional of the electron density. *Physics Review. B, Condensed Matter*, 37(2), 785–789.
- MolSoft, I. (2000). 2.8 Program manual. San Diego, CA: MolSoft LLC.
- Molsoft, L. L. C. "ICM-browser." MolsoftInc, San Diego (2017).
- Neves, M. A., Totrov, M., and Abagyan, R. (2012). Docking and scoring with ICM: the benchmarking results and strategies for improvement. *Journal of Computer-aided Molecular Design*, 26(6), 675-686.
- Patterson, C. M., Balachander, S. B., Grant, I., Pop-Damkov, P., Kelly, B., McCoull, W., Parker, J., Giannis, M., Hill, K. J., Gibbons, F. D., Hennessy, E. J., Kemmitt, P., Harmer, A. R., Gales, S., Purbrick, S., Redmond, S., Skinner, M., Graham, L., Secrist, J. P., Schuller, A. G., Wen, S., Adam, A., Reimer, C., Cidado, J., Wild, M., Gangl, E., Fawell, S. E., Saeh, J., Davies, B. R., Owen, D. J. and Ashford, M. B. (2021). Design and optimisation of dendrimer-conjugated Bcl-2/x_L inhibitor, AZD0466, with improved therapeutic index for cancer therapy. *Communications Biology*, 4(1), 112.
- Phillips, J. C., Hardy, D. J., Maia, J. D. C., Stone, J. E., Ribeiro, J. V., Bernardi, R. C., Buch, R., Fiorin, G., Hémin, J., Jiang, W., McGreevy, R., Melo, M. C. R., Radak, B. K., Skeel, R. D., Singharoy, A., Wang, Y., Roux, B., Aksimentiev, A., Luthey-Schulten, Z., Kalé, L. V., Schulten, K., Chipot, C. and Tajkhorshid, E. (2020). Scalable molecular dynamics on CPU and GPU architectures with NAMD. *The Journal of Chemical Physics*, 153(4), 044130. <https://doi.org/10.1063/5.0014475>
- Rooswinkel, R.W., Van-de Kooij, B., de Vries, E., Pauwe, M., Braster, R., Verheil, M., and Borst, J. (2014). Antiapoptotic potency of Bcl-2 proteins primarily relies on their stability, not binding selectivity. *Blood, The Journal of American Society of Hermatology*, 123(18), 2806-2815
- Scarpino, A., Ferenczy, G. r. G., and Keserü, G. r. M. (2018). Comparative evaluation of covalent docking tools. *Journal of Chemical Information and Modeling*, 58(7), 1441-1458.
- Singh, R., Letai, A., and Sarosiek, K. (2019). Regulation of apoptosis in health and disease: The balancing act of Bcl-2 family proteins. *Nature Reviews Molecular Cell Biology*, 20(3), 175-193.
- Speck-Planche, A., Kleandrova, V. V., Luan, F., and Cordeiro, M. N. D. (2012). Rational drug design for anti-cancer chemotherapy: multi-target QSAR models for the in silico discovery of anti-colorectal cancer agents. *Bioorganic and Medicinal Chemistry*, 20(15), 4848-4855.
- Thomsen, R. and Christensen, M.H. (2006). MolDock: A new technique for high-accuracy molecular docking. *Journal of Medicinal Chemistry*, 49(11), 3315-3321
- Tinworth, C.P., and Young, R.J. (2020). Facts, patterns, and principles in drug discovery: Appraising the rule of 5 with measured physicochemical data. *Journal of Medicinal Chemistry*, 63(18), 10091-10108
- Warren, C. F., Wong-Brown, M. W., and Bowden, N. A. (2019). Bcl-2 family isoforms in apoptosis and cancer. *Cell Death and Disease*, 10(3), 1-12.
- Zhang, J. (2009). Studies on the structural stability of rabbit prion probed by molecular dynamics simulations. *Journal of Biomolecular Structure and Dynamics*, 27(2), 159-162.
- Zhang, Q., Riley-Gillis, B., Han, L., Jia, Y., Lodi, A., Zhang, H., Sweeney, S. R. (2022). Activation of Ras/Mapk pathway confers Mcl-1 mediated acquired resistance to Bcl-2 inhibitor venetoclax in acute myeloid leukemia. *Signal Transduction and Targeted Therapy*, 7(1), 1-13.

Publisher's Note: All claims expressed in this article are solely those of the authors and do not necessarily represent those of their affiliated organizations, or those of the publisher, the editors and the reviewers. Any product that may be evaluated in this article, or claim that may be made by its manufacturer, is not guaranteed or endorsed by the publisher. The publisher remains neutral with regard to jurisdictional claims.

Copyright © 2022 by Arthur et al. This is an open-access article distributed under the terms of the Creative Commons Attribution License (CC BY). The use, distribution or reproduction in other forums is permitted, provided the original author(s) and the copyright owner(s) are credited and that the original publication in this journal is cited, in accordance with accepted academic practice. No use, distribution or reproduction is permitted which does not comply with these terms.



Submit your next manuscript to NJBMB at
<https://www.nsbmb.org.ng/journals>